19th Australasian Fluid Mechanics Conference
Melbourne, Australia
8-11 December 2014

Reynolds Number Influence on the Vortex-Induced Vibration Critical Point of a Pivoted Cylinder

B. Stappenbelt and A. Johnstone

School of Mechanical, Materials and Mechatronic Engineering
University of Wollongong, Wollongong, New South Wales 2522, Australia

Abstract

The aim of the present investigation was to examine the Reynolds number dependence of the critical vortex-induced vibration (VIV) point for cylinders in a pivoted system. For translational systems, the existence of a critical mass ratio for cylinders undergoing vortex-induced vibration has been well established. At mass ratios below this critical point, the reduced velocity at VIV lock-out tends to infinity, resulting in the resonance forever condition as described by the authors first reporting this phenomenon. For translating cylinder VIV, a Reynolds number dependence of the critical mass ratio has been noted. A variation of the critical mass ratio from 0.36 at low Reynolds number, tending toward 0.54 at higher values has been observed. To the author's knowledge, no such Reynolds dependence has previously been reported for pivoted cylinders. The approach adopted in the present investigation involved measuring the VIV response of a positively buoyant pivoted cylinder being towed at very high reduced velocity at different Reynolds numbers. High reduced velocity was attained by establishing a very low system natural frequency and the Reynolds number was controlled via the towing velocity and the cylinder diameter. The key finding of this study is a Reynolds number dependence of the critical force moment ratio in the pivoted cylinder arrangements with values similar to that of the critical mass ratio in translational systems. Over the Reynolds range of experimentation (5.3×10^3 to 6.5×10^4), the critical force moment ratio varied from 0.43 to 0.53.

Introduction

Fluid flow past a circular cylindrical object generates vorticity due to the shear present in the boundary layer. This vorticity in the flow field coalesces into regions of concentrated vorticity, known as vortices, on either side of the cylinder. Flow above a threshold Reynolds number allows perturbations in the flow upstream to cause one of the vortices to grow larger. This vortex, with higher flow velocities and accompanying lower pressures, draws the smaller vortex from the opposing side across the wake centreline. The opposite vorticity from this smaller vortex severs the vorticity supply of the larger vortex, allowing it to convect downstream [20]. This process is repeated in the reverse sense, leading to alternating vortex shedding from the cylinder.

When the cylinder is elastically restrained and natural frequencies are introduced, a fluid-elastic instability known as vortex-induced vibration (VIV) results. The time-varying non-uniform pressure distribution around the cylinder resulting from the vortex shedding causes structural vibrations both inline and transverse to the flow. Near the natural frequency of the structure, the vortex-shedding frequency synchronises with the natural frequency and the vibration frequency. One of the primary mechanisms responsible for this synchronisation is the change in hydrodynamic mass, as demonstrated in the experiments of Vikestad [21]. The range of reduced velocity over which this synchronisation occurs is known as the lock-in range. Mostly, the ensuing vibrations are undesirable, resulting in increased fatigue loading and component design complexity to accommodate these motions. The transverse vibrations also result in higher dynamic relative to static drag coefficients.

With decreasing mass ratio, an increase in the amplitude response is generally evident [17]. Also, the smaller the mass ratio, the larger the relative influence of the hydrodynamic mass on the vibration response of the structure.

Various definitions for the mass ratio are widely employed. In this work, the mass ratio is defined as the ratio of the oscillating structural mass, m, to the displaced fluid mass, m_d, as

$$\mathrm{m}^* = \frac{\mathrm{m}}{\mathrm{m_d}}. \tag{1}$$

The structural mass, m, includes any enclosed fluid, but excludes the hydrodynamic mass. Note that the mass ratio is equivalent to the magnitude of the ratio of the weight, W, and buoyancy, B, forces since

$$\mathrm{m}^* = \frac{\mathrm{W}}{\mathrm{B}} = \frac{\mathrm{mg}}{\mathrm{m_d g}}. \tag{2}$$

The mass ratio parameter influences both the amplitude and frequency response of the cylinder. With higher mass ratios (e.g. a cylinder vibrating in air, with a mass ratio $O(100)$), changes in added mass are relatively insignificant due to the low density of the fluid. The natural frequency then remains relatively unchanged throughout the lock-in range. When the fluid medium under consideration is much denser (e.g. a cylinder vibrating in water), distinct changes in the natural frequency are observed. The increasing natural frequency observed with increasing reduced velocity is directly attributable to the decreasing added mass throughout the lock-in range [18, 21]. An overview of the characteristics of low mass damping VIV is given in the review paper by Gabbai & Benaroya [2].

Since the hydrodynamic mass variation is largely responsible for synchronisation of the shedding and vibration frequencies, typically much wider lock-in regions are experienced at low mass ratio [17, 21]. The limit of this trend is found at the critical mass ratio of around 0.54 [5], below which there exists no lock-out point and VIV occurs at all velocities above the initial lock-in. This is the resonance forever condition as described by the authors first reporting this phenomenon.

Using the approach adopted by Khalak and Williamson [10] a frequency equation may be obtained by substituting harmonic force and response expressions in the forced linear oscillator equation of motion. The resulting frequency equation, the ratio of vibration frequency to the system natural frequency, is

$$f^* = \frac{f}{f_n} = \sqrt{\frac{m^*+C_A}{m^*+C_{EA}}} \quad (3)$$

where C_A is the potential added mass coefficient (equal to one for a circular cylinder) and C_{EA} is the effective added mass coefficient which is related to the force in phase with acceleration.

Govardhan and Williamson [3] discovered that in the lower VIV response branch the effective added mass was approximately constant at a value of $C_{EA} = -0.54$. The frequency equation (equation 3) then becomes

$$f^* = \sqrt{\frac{m^*+1}{m^*-0.54}}. \quad (4)$$

From equation 4, it is clear then, that with small mass ratio, approaching the value of 0.54, a large frequency ratio results for the lower VIV response branch. As the mass ratio approaches the critical value of m_{crit} = 0.54, the frequency ratio tends to infinity and consequently the lower branch can never be reached. The upper VIV response branch then continues indefinitely, resulting in the infinite resonance regime. The lower response branch essentially ceases to exist below the critical mass ratio.

The initial discovery of the critical mass ratio resulted from the examination of elastically constrained cylinder experimental data[3]. Subsequent transverse amplitude tests on translational cylindrical systems where restoring forces have been removed (i.e. with the reduced velocity, $U_r \rightarrow \infty$) have been conducted [4]. At very high reduced velocity (i.e. as $U_r \rightarrow \infty$) resonance is seen below the critical mass ratio. Above the critical mass ratio, smaller amplitude forced vibrations are evident. The development of understanding of the critical mass ratio for a single degree of freedom cylindrical system is chronicled well in the publications by Govardhan and Williamson [4, 5] in which a critical mass ratio 0.542 ± 0.01 is claimed.

The Reynolds number has been shown to have a significant effect on the maximum response amplitude as reported by Govardhan and Williamson [6] and Klamo, Leonard and Roshko [11]. These Reynolds number dependencies were characterised in more detail in the later work by Govardhan and Williamson [7]. The low Reynolds number study by Ryan, Thompson and Hourigan [15] also revealed a Reynolds number dependency of the critical mass ratio. This was supported by the study by Morse and Williamson [13] which showed an increase in critical mass ratio from 0.36 to 0.54 over the Reynolds number range of 4 x 10^3 to 3 x 10^4 as illustrated in figure 1.

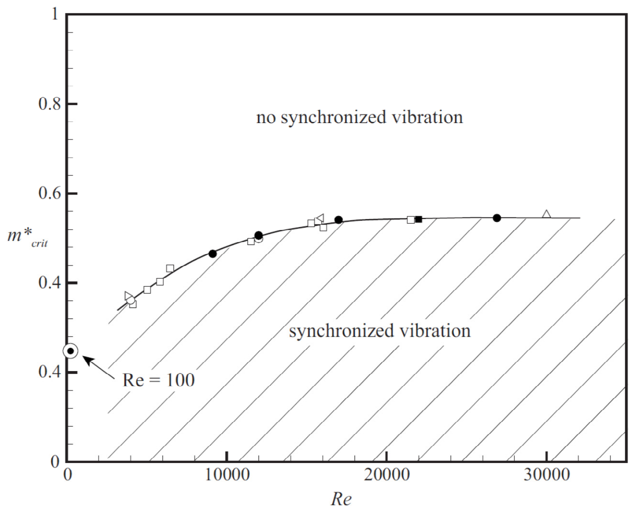

Figure 1. Critical mass ratio dependence on Reynolds number [13]

The investigation by Horowitz and Williamson [8] where the VIV motions of a rising and falling cylinder were examined yielded a critical mass ratio of 0.54. This arrangement, despite allowing the cylinder multiple degrees of freedom, produced results in close agreement with previous experiments. A system free to vibrate inline and transverse to the flow has the potential at low mass ratio to display a super-upper response branch (e.g. Pesce and Fujarra, [14] and Stappenbelt & Lalji, [16]) rather than the upper response branch observed in transverse only experiments. By extrapolation of their data, the two degree of freedom system experiments by Jauvtis and Williamson [9] revealed a critical mass ratio value of 0.522.

Few published studies have examined the critical point for a pivoted cylinder. The studies by Leong and Wei [12] and Voorhees, Dong, Atsavapranee, Benaroya and Wei [22] attempt to apply the concept of the mass ratio to a rotational system. Insufficient information is provided in these papers to ascertain the mass moment of inertia of the cases covered. The former study presents only partial response curves for limited mass ratios and the latter only provides experimental results above the critical point.

In the pivoted cylinder study by Flemming and Williamson [1] the mass moment of inertia ratio is surmised, using the approach by Khalak and Williamson [10], to be the governing parameter for the VIV critical point. Adopting the mass moment of inertia ratio as the governing parameter appears to be the logical choice as it is the rotational analogy of the mass ratio in a translational system. In the investigation by Flemming and Williamson [1], three mass moment of inertia ratio cases were covered, ranging from I^*=7.69 to I^*=1.03. These experiments, although all performed above the critical point, yielded effective added inertia coefficient (C_{EAI}) data that allowed a prediction of a critical point value of $I^*_{crit} \approx 0.5$. It must be noted however that the C_{EAI} values obtained were not constant in the lower response branch (as was the case for C_{EA} values for the translating cylinders), rather, they were continually decreasing until the de-coherence region.

The force moment ratio, M^*, is defined as the ratio of the moment about the point of rotation due to the weight force acting on the structural mass to that acting on the displaced fluid mass as

$$M^* = \frac{M}{M_d}. \quad (5)$$

Note that equation 5 is equivalent to the magnitude of the ratio of moments due to the structural weight (i.e. $W.r_w.sin\theta$ where r_w is the distance of the centre of gravity (CoG) to the centre of rotation) and buoyancy (i.e. $B.r_B.sin\theta$ where r_B is the distance of the centre of buoyancy (CoB) to the centre of rotation) forces in the plane of transverse oscillations,

$$\text{i.e. } M^* = \left|\frac{Wr_W \sin\theta \sin\alpha}{Br_B \sin\theta \sin\alpha}\right| = \left|\frac{Wr_W}{Br_B}\right|. \quad (6)$$

The study by Stappenbelt and Johnstone [19] showed the existence of a critical point for a pivoted cylinder which was governed by the force moment ratio rather than the mass moment of inertia ratio. The aim of the present study is to examine the dynamics of a pivoted cylinder to determine the Reynolds number dependence of the critical point for rotational systems.

Methodology

The present investigation consists of an experiment in which a pivoted cylinder as illustrated in the sketch of figure 2 was towed along a 32.5m water tank. Inline vibrations were restrained and transverse vibrations were measured by the use of laser displacement transducers. Figure 2 also acts as a parameter definition sketch. The angular displacement relative to the initial position of the cylinder in the plane of transverse oscillation is designated θ. It is the angular position relative to the vertical.

Table 1 details the parameter values for the experiment. The force moment ratio was experimentally controlled by the addition of lump masses inside the end of the cylinder. The experiment was conducted over a Reynolds number range from 5.3 x 10^3 to 6.5 x 10^4.

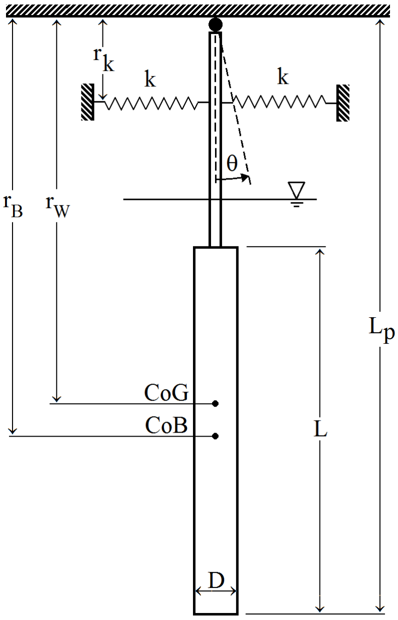

Figure 2 Experimental apparatus and parameter definition sketch.

The approach adopted in the present study to determine the location of the critical point was to examine the nature of the vortex-induced vibrations at very high reduced velocity (i.e. as $U_r \to \infty$). The amplitude of the response indicated either resonant (i.e. below the critical point) or forced vibration (i.e. above the critical point).

Parameter	Symbol	Value
Force moment ratio range	M^*	0.315-0.762
Reynolds number range	Re	5.3×10^3-6.5×10^4
Cylinder length	L	842 mm
Pivoted length	L_p	1256 mm
Cylinder diameter	D	48 mm
Structural damping ratio	ζ	0.006
Minimum reduced velocity	U_r	$O(1000)$

Table 1 Experimental parameter values.

The non-dimensionalised freestream flow velocity (i.e. the reduced velocity) is given by

$$U_r = \frac{U}{f_n D}. \quad (7)$$

The natural frequency, f_n, is proportional to the square root of the angular restoring force coefficient, k_θ. Considering the sum of the moments about the cylinder pivot point it may be shown that

$$k_\theta = W r_W - B r_B + 2 k r_k. \quad (8)$$

To test for resonance as $U_r \to \infty$, the restoring force coefficient, k_θ, must tend to zero. From equation 8 it may be seen that this condition is approached as

$$k r_k \to (W r_W - B r_B)/2. \quad (9)$$

The spring rate and distance of the point of restoring force action from the pivot were utilised to ensure that the reduced velocity was always of the order of 1000. Some restoring capability was of course necessary to maintain the centralising tendency of the cylinder whilst undergoing flow induced vibration.

Results

Two time series samples are provided in figure 3. The angular displacements in these plots are normalised by the angle θ_D equal to half the angle subtended in the arc defined by a chord and radius equal to the diameter and length from the cylinder tip to pivot point respectively. The time series obtained in this study typically displayed a low frequency drift from the equilibrium position due to the low restoring tendency of the system with $k_\theta \to 0$.

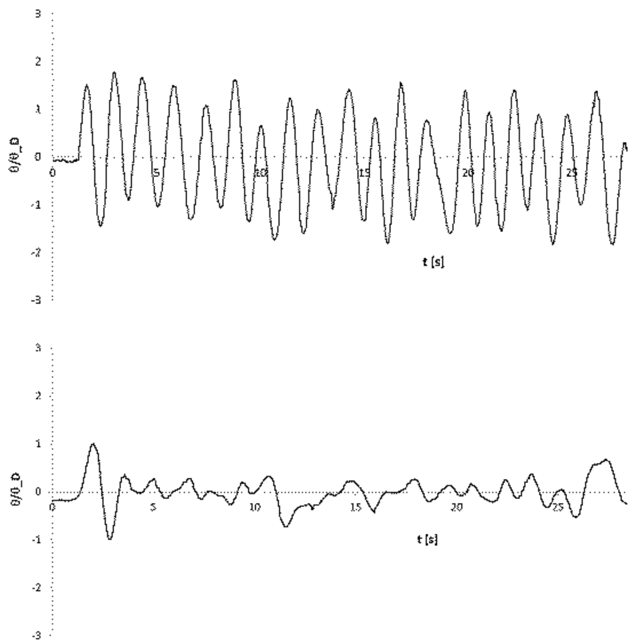

Figure 3. Time response above (a) M^*=0.33 and below (b) M^*=0.70 the critical point: Re=1.2 x 10^4.

It is clear from figure 3 that a transition from low amplitude forced vibration response to high amplitude resonant response occurs indicating the critical point. Figure 3a is an example of the nature of the resonant vibrations below the critical point displaying large amplitude regular oscillations. This is in contrast with figure 3b which is an example of the forced vibration response of the pivoted cylinder above the critical point.

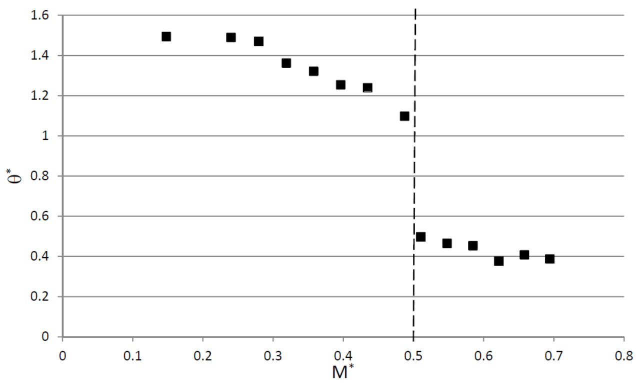

Figure 4. Response amplitude as a function of the force moment ratio at Re=3.16 x 10^4.

The angular response of the cylinder at various force moment ratios at a Reynolds number of 3.16 x 10^4 are presented in figure 4. Each data point in these plots represents the averaged half peak to peak angular response of between 60 and 85s of steady-state data collected, representing between 52 and 58 oscillation periods. The angular displacement amplitude is normalised as

$$\theta^* = \frac{\theta_{max}}{\theta_D}. \quad (10)$$

The transition from resonant to forced vibration appears to occur at M^*=0.504 implying the occurrence of the critical point in this region. This process was repeated at 24 different Reynolds numbers ranging from 5.3 x 10^3 to 6.5 x 10^4. The cirtical points, identified through the forced to resonant amplitude transitions, at these Reynold numbers are plotted in figure 5.

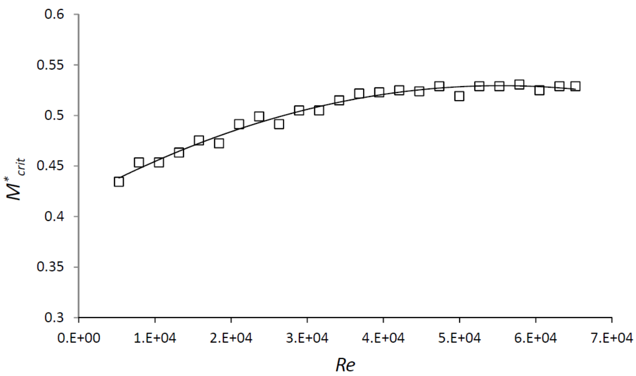

Figure 5. Pivoted-system critical-point variation with flow Reynolds number.

Conclusions

It is clear from figure 5 that there exists a Reynolds number dependence of the critical vortex-induced vibration point of a pivoted cylinder. The form of this dependence is analogous to that reported for translating cylinders (e.g. the work by Morse and Williamson [13] in figure 1).

The asymptotic behaviour of the critical point at higher Reynolds number noted in the translating cylinder case is also observed in the present case. The critical force moment ratios for pivoted cylinders tend to 0.53 with increasing Reynolds number, corresponding reasonably well with the translating cylinder critical point values reported.

Acknowledgements

The authors gratefully acknowledge the contribution to this work by Mr. Matthew Vassallo and Mr. Ashley Heath during their undergraduate research project at the University of Wollongong.

References

[1] Flemming, F & Williamson, C H K 'Vortex-Induced Vibrations of a Pivoted Cylinder', *Journal of Fluid Mechanics*, vol.522, 2005, pp215-252.

[2] Gabbai, R D & Benaroya, H 'An overview of modelling and experiments of vortex-induced vibration of circular cylinders', *Journal of Sound and Vibration*, vol.282, no.3-5, 2005, pp575-616.

[3] Govardhan, R. & Williamson, C. H. K. Modes of vortex formation and frequency response of a freely vibrating cylinder. *J. Fluid Mech.* 420, 2000, pp. 85-130.

[4] Govardhan, R & Williamson, C H K Resonance forever: existence of a critical mass and an infinite regime of resonance in vortex-induced vibration, *Journal of Fluid Mechanics*, vol.473, 2002, pp147-166.

[5] Govardhan, R & Williamson, C H K Critical Mass in Vortex-Induced Vibration of a Cylinder, *European Journal of Mechanics, B/Fluids*, vol.23, no.1, 2004, pp17-27.

[6] Govardhan R. & Williamson, C. H. K. Revealing the effect of Reynolds number on vortex-induced vibrations using controlled negative and positive damping, *Proceedings of the Fourth Conference on Bluff Body Wakes and Vortex-Induced Vibration (BBVIV-4)*, 2005.

[7] Govardhan R. & Williamson, C. H. K. Defining the 'modified Griffin plot' in vortex-induced vibration: Revealing the effect of Reynolds number using controlled damping, *J. Fluid Mech.,* Vol. 561, 2006, p. 147.

[8] Horowitz, M & Williamson, C H K Dynamics of a Rising and Falling Cylinder, *Journal of Fluids and Structures*, vol.22, no.6-7, 2006, pp837-843.

[9] Jauvtis, N & Williamson, C H K The Effect of Two Degrees of Freedom on Vortex-Induced Vibration at Low Mass and Damping, *Journal of Fluid Mechanics*, vol.509, 2004, pp23-62.

[10] Khalak, A. & Williamson, C. H. K. Motions, forces and mode transitions in vortex-induced vibrations at low mass-damping, *J. Fluids Struct.* Vol. 13, 1999, p. 813.

[11] Klamo, J. T., Leonard, A. & Roshko, A. On the maximum amplitude for a freely vibrating cylinder in cross-flow, *J. Fluids Struct*. Vol. 21, 2005, p. 429.

[12] Leong, C M and Wei, T Two-Degree-of-Freedom Vortex-Induced Vibration of a Pivoted Cylinder below Critical Mass Ratio, *Proceedings of the Royal Society A: Mathematical, Physical and Engineering Sciences*, vol.464, no.2099, 2008, pp2907-2927.

[13] Morse, T. & Williamson, C. The effect of Reynolds number on the critical mass phenomenon in vortex-induced vibration, *Physics of Fluids*, 21, 2009.

[14] Pesce, C, and Fujarra, A The Super-upper Branch VIV Response of Flexible Cylinders, *BBVIV4, Conf Bluff Body Wakes and Vortex-Induced Vibrations*, 2005.

[15] Ryan, K., Thompson, M. & Hourigan, K. Variation in the critical mass ratio of a freely oscillating cylinder as a function of Reynolds number, *Physics of Fluids*, 17, 2005.

[16] Stappenbelt, B. & Lalji, F. Vortex-induced vibration super-upper response branch boundaries, *International Journal of Offshore and Polar Engineering,* Vol. 18, No. 2, 2008, pp. 99-105.

[17] Stappenbelt, B, and O'Neill, L Vortex-induced Vibration of Cylindrical Structures with Low Mass Ratio, *Proc 17th International Offshore and Polar Eng Conference*, 2007.

[18] Stappenbelt, B. Vortex-Induced Motion of Nonlinear Offshore Structures: A study of catenary moored system fluid-elastic instability, *LAP Lambert Academic Publishing*, 2010.

[19] Stappenbelt, B. & Johnstone, A. The critical point in the vortex induced vibration of a pivoted cylinder, *International Journal of Offshore and Polar Engineering,* Vol. 23, No. 3, 2013, pp. 205-209.

[20] Sumer, BM, and Fredsoe, J Hydrodynamics Around Cylindrical Structures, *World Scientific Publishing Co. Pte. Ltd.*, London, 2007.

[21] Vikestad, K Multi-frequency Response of a Cylinder Subjected to Vortex Shedding and Support Motions, *PhD Thesis, Norwegian Univ of Sci and Tech, Trondheim*, 1998.

[22] Voorhees, A, Dong, P, Atsavapranee, P, Benaroya, H & Wei, T Beating of a Circular Cylinder Mounted as an Inverted Pendulum, *Journal of Fluid Mechanics*, vol. 610, 2008, pp 217-247.